Supporting Information

Porous Titanium Oxynitride Sheets as Electrochemical Electrodes for Energy Storage

*Ting-Ting Chen,[a] Hsiao-Ping Liu,[a] Yen-Ju Wei,[b] I-Chun Chang,[a] Min-Han Yang,[a] Yu-Shu Lin,[a] Kuei-Lin Chan,[a] Hsin-Tien Chiu,[b] and Chi-Young Lee[a]**

[a]Department of Materials Science and Engineering, National Tsing Hua University, Hsinchu 30013, Taiwan, R. O. C.

[b]Department of Applied Chemistry, National Chiao Tung University, Hsinchu 30010, Taiwan, R.O.C.

*Corresponding author
Chi-Young Lee
Department of Materials Science and Engineering,
National Tsing Hua University,
101, Sec. 2, Kuang-Fu Road, Hsinchu 30013,Taiwan, R. O. C.
e-mail cylee@mx.nthu.edu.tw
TEL: 886-3-5728692
FAX: 886-3-5722366

Supporting Information

Experiment

Preparation of TiO_xN_y sheets

In a typical experiment, 0.2 g of TiO_2 powder (Degussa P25) was introduced into 30 ml of 10 M NaOH solution in a Teflon-lined autoclave, and the hydrothermal reaction performed in a furnace over 48 hours at 195 °C. After that, the sodium titanate powder was collected and casted on the membrane (FP-2000TM, pore size: 0.45μm) during filtering by a water pump, followed by rinsing with distilled water and 0.5 M nitric acid to further exchange sodium ions by hydrogen ions. After being dried at 50 °C on the oven overnight, the titanate sheet (ST) was obtained due to the separation from the filter membrane during the evaporation of water.

ST sheets were heated at different temperature (600 °C, 700 °C, and 800 °C) under ammonia atmosphere ($NH_{3(g)}$, flow rate: 40 sccm, Sanyingas, 99.9%) for 4h/8h in a horizontal quartz-tube furnace with a slow heating rate (2 °C min^{-1}). After the nitridation process, the white sheet changed their colour to dark. The sample prepared at 600 °C for 4 h, 700 °C for 4 h, and 800 °C for 4 h and 8h were named as N64, N74, N84 and N88 respectively. For comparison, ST sheet was heated at 700 °C for 1 h under air and the resulting product was named as O71.

Characterization of TiO_xN_y sheets

The X-ray diffraction (XRD) pattern was recorded on a BRUKER AXS D8 ADVANCE, a Bragg-Brentano-type diffractometer with Cu $K\alpha_1$ radiation. Celref software was employed to evaluate their lattice parameter by refining the corresponding XRD patterns. Scanning electron microscopy (SEM) was conducted on a JSE-6500F field emission microscopy from JEOL. Crystallinity and morphology details of the powders were investigated using the transmission electron microscope (TEM, JEOL 200 CX). X-ray Photoelectron Spectroscopy (XPS) was conducted on a PHI Quantera Spectrometer (ULVAC-PHI). Brunauer-Emmett-Teller (BET) surface area measurements were performed on a micrometrics ASAP 2020 (All the products were preheated to 80 °C under vacuum for degasification). The conductivity was evaluated by using Hall Effect Measurement System (Ecopia, HMS-3000).To investigate the electrochemical performance of the as-synthesized products, cyclic voltammetry (CV) tests and galvanostatic (GV) charge/discharge tests in 2 M H_2SO_4 were performed on a three-electrode cell system by an Autolab PGSTAT302N. The trimmed TiO_xN_y sheet placed on a FTO glass was served as a working electrode. A Pt-wire and an Ag/AgCl electrode were used as the counter and the reference electrodes, respectively.

Supporting Information

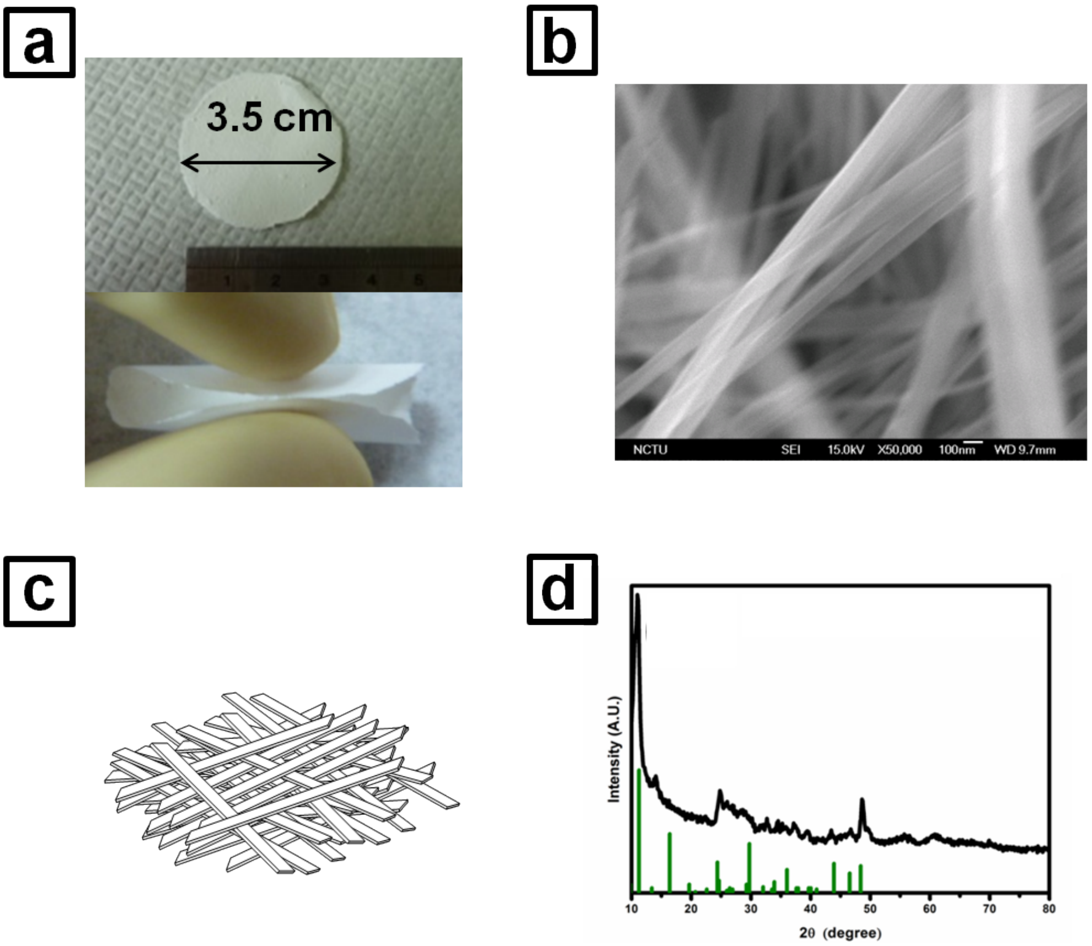

Fig. S1 (a) photographs (b) SEM image (c) scheme (d) XRD pattern of the ST sheet. A ST sheet was composed of densely and randomly stacked titanate fibers. The randomly fibers have intertwined into voids (typically ~80 nm). Fig. S1c shows the scheme of the voids between randomly intertwined fibers. Fig. S1d shows the XRD pattern of ST which matches the standard pattern of $H_4Ti_4O_{10}$ (JCPDS 38-0699) well.

Supporting Information

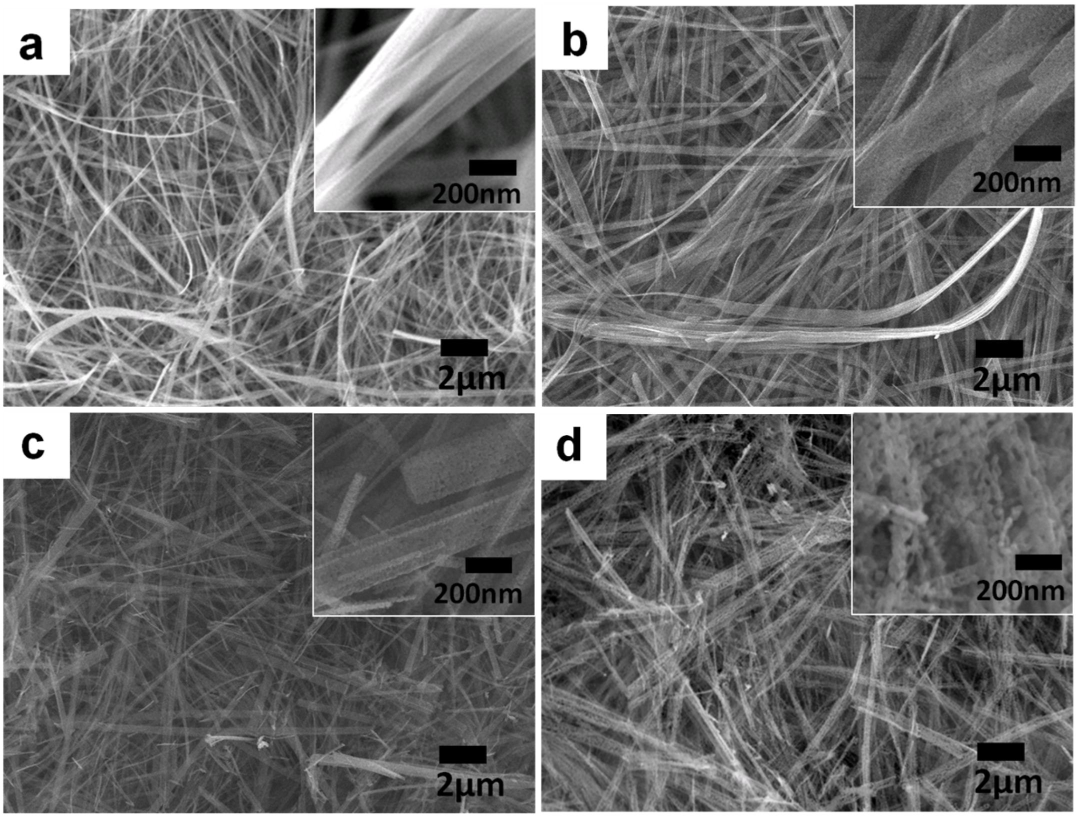

Fig. S2 SEM images of as-synthesized products: (a) ST (b) N64 (c) N74 (d) N84

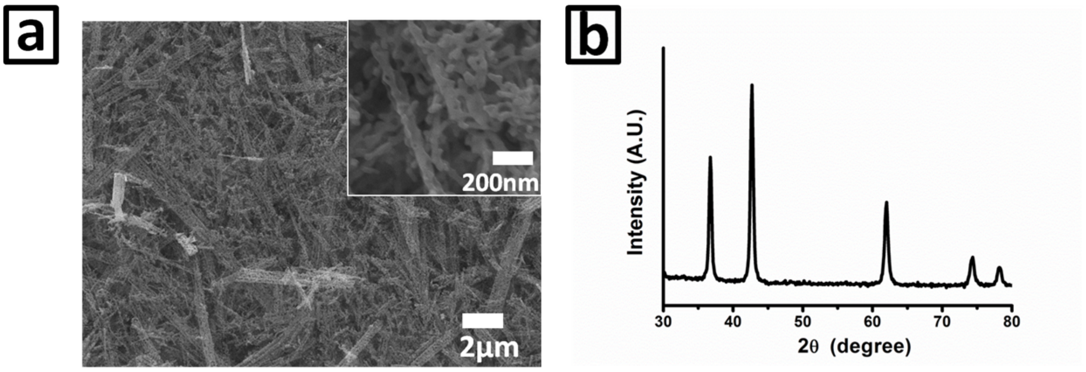

Fig. S3. (a) SEM image (b) XRD pattern of N88.

Supporting Information

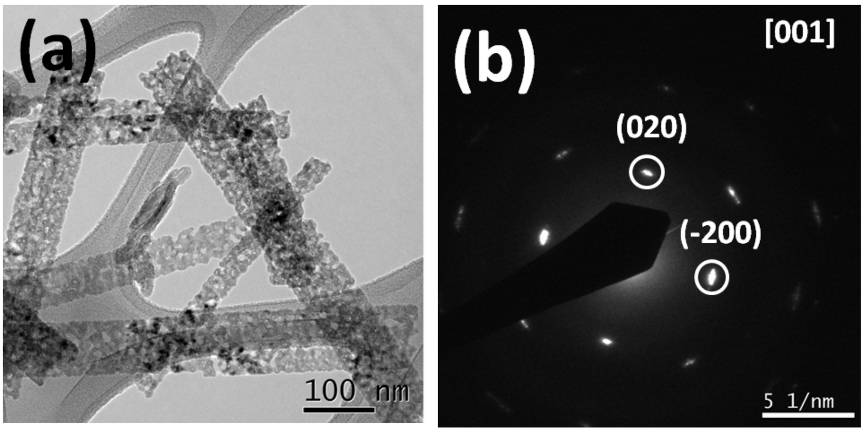

Fig. S4 TEM studies of N64 (a) Low-magnification image and (b) SAED

Supporting Information

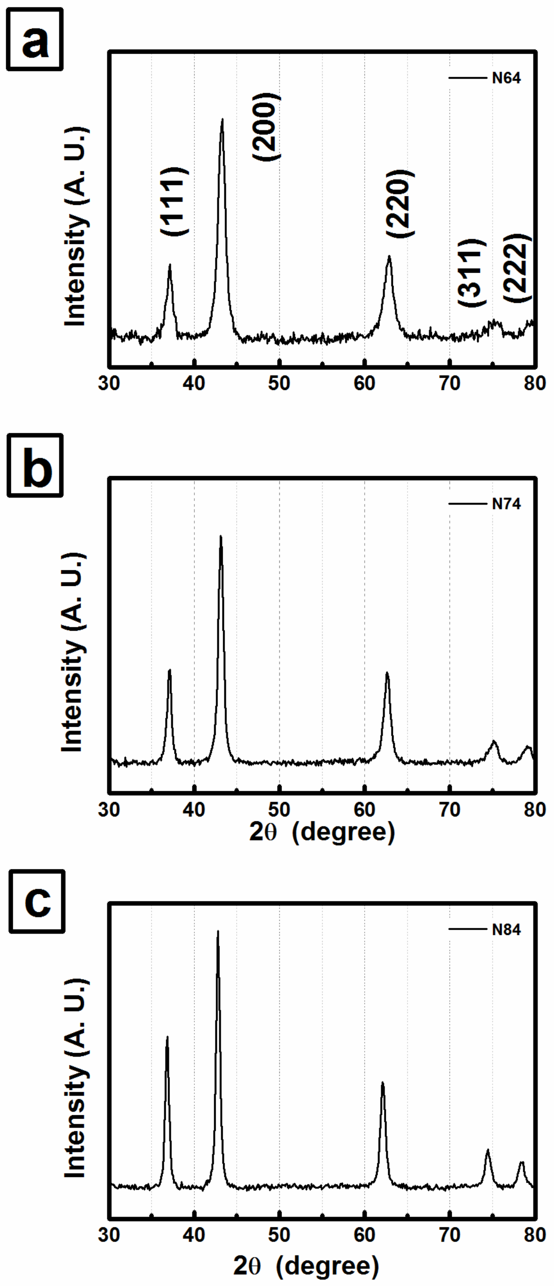

Fig. S5 XRD patterns of TiO_xN_y sheets: (a) N64 (b) N74 (c) N84.

Supporting Information

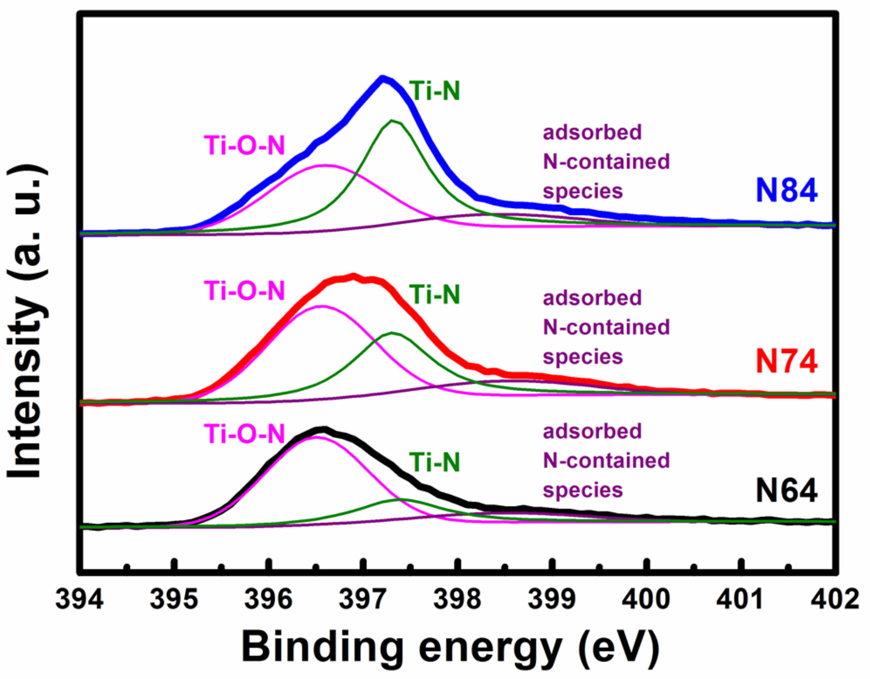

Fig. S6 XPS spectra of N1s for N64, N74, and N84. The two major peaks, 396.5 and 397.3 eV are attibuted to TiO_xN_y and TiN respectivly, whereas the small peak at 398.5 is adsorbed N-contained species.

Supporting Information

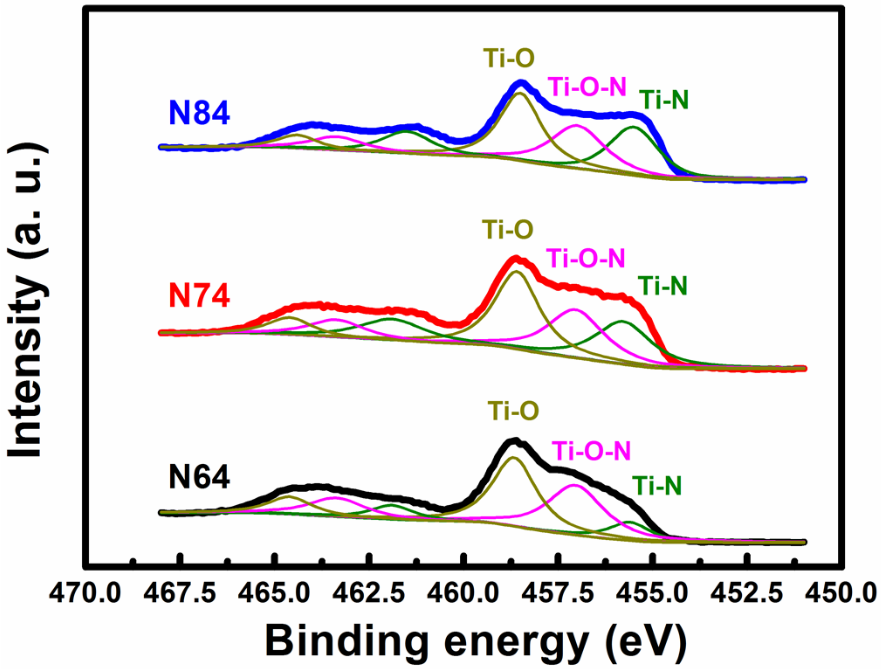

Fig. S7 XPS spectra of Ti 2p for N64, N74, and N84. The detection of TiO_2 (Ti-O bonding) is attributed to the "amorphous TiO_2" due to oxide that was caused by the exposure of the samples to air before the XPS measurement (crystalline TiO_2 was not found by XRD). Hence, XPS could not prove unequivocally stoichiometry analysis of O/N ratio in TiN_xO_y.

Supporting Information

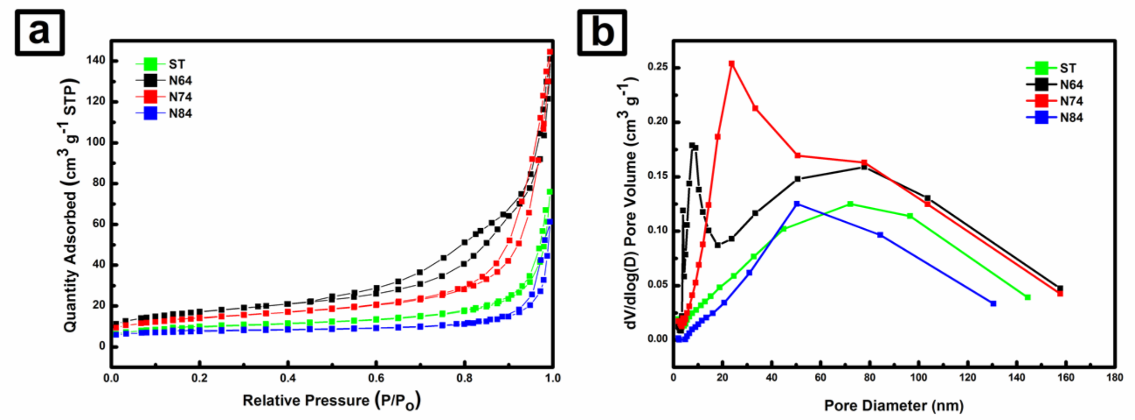

Fig. S8 (a) Nitrogen adsorption and desorption isotherms of as-synthesized products and (b) their pore-size distribution obtained from adsorption branch of isotherm using BJH method. The presence of mesopores was found in N64 and N74. ST and TiO_xN_y had a pore size of~ 80 nm which is corresponding to micropores.

Supporting Information

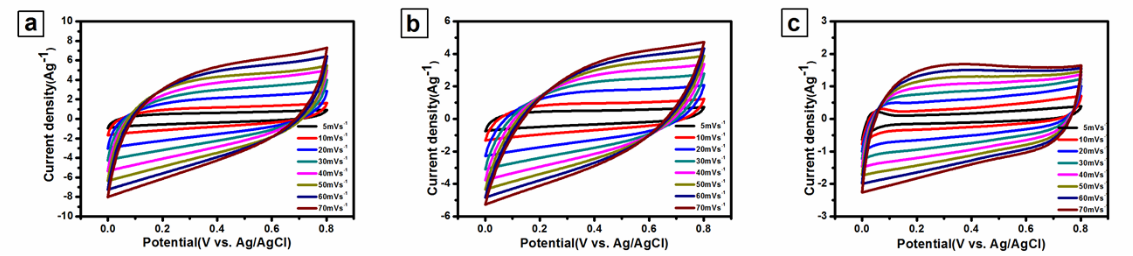

Fig. S9 CVs curves of TiO_xN_y electrodes at different scan rates of 5 to 70 mVs^{-1}: (a) N64, (b) N74 ,(c) N84.

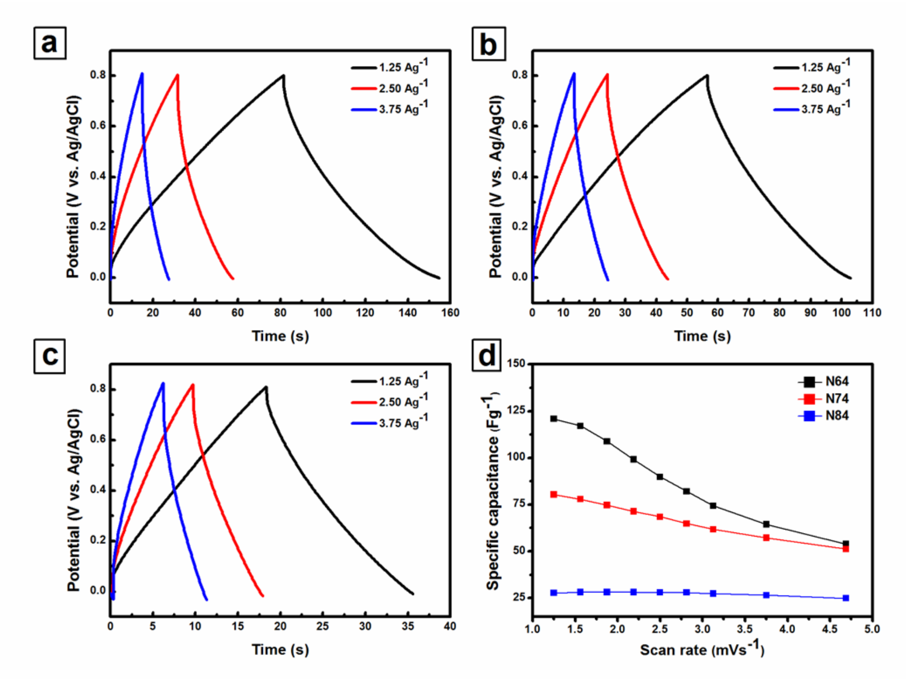

Fig. S10 Constant current charge/discharge curves of TiO_xN_y electrodes at different current density 1.25 to 3.75 Ag^{-1}: (a) N64, (b) N74, and (c) N84. (d) rate-dependent GVs of TiO_xN_y electrodes at various current densities.

Supporting Information

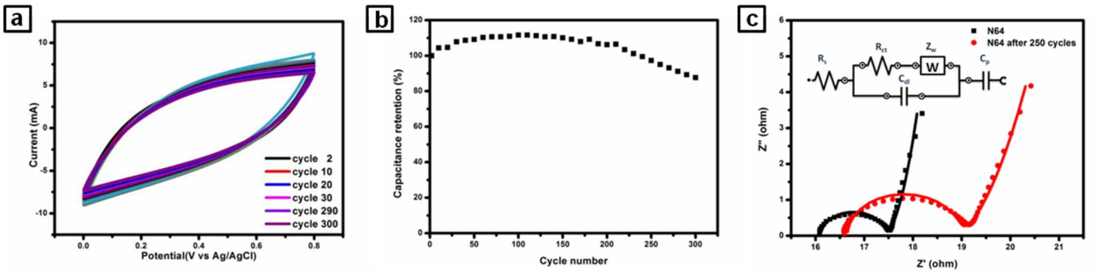

Fig. S11 (a) CVs of N64 electrode with scan rate of 70 mVs^{-1} over 300 cycles. (b) Calculated capacitance retention of N64 as a function of cycling number. (c) Nyquist plots of N64 electrode with an amplitude of 5 mV over a frequency from, 1 Hz to10^5 Hz and the corresponding equivalent circuit. The specific capacitance of the electrode reveals a decay of 12% after 300 cycles. Fig. S11c shows that R_s and R_{ct} are slightly increased in the sample after 250 charge/discharge cycles. This probably results from the formation of less active and insulated TiO_2 which will be formed during irreversible electrochemical oxidation of TiO_xN_y.[1] The increased R_{ct} and R_s are responsible for the decay of specific capacitance in the stability test.

Reference:

[1] X. Lu, G. Wang, T. Zhai, M. Yu, S. Xie, Y. Ling, C. Liang, Y. Tong and Y. Li, *Nano Lett.*, 2012, **12**, 5376.

Supporting Information

Table S1. Performance of TiN-based supercapacitor

Materials	Electrolyte	C_{sp} (F g^{-1})	Condition	Ref.
PANI/TiN	1 M HCl	80	5 mV s^{-1}	[1]
TiN microspheres	1 M $LiPF_6$	133	2 mV s^{-1}	[2]
TiN fibers	1 M KOH	145	2 mVs^{-1}	[3]
TiN nanowire	1 M KOH	123	10 mV s^{-1}	[4]
TiN_xCl_y	1 M KOH	238	2 mV s^{-1}	[5]
TiO_xN_y	1 M H_2SO_4	120.9	1.25 A g^{-1}	This work

Reference:

[1] Y. Qiu and L. Gao, *J. Phys. Chem. B*, 2005, **109**, 19732.

[2] S. Dong, X. Chen, L. Gu, X. Zhou, H. Xu, H. Wang, Z. Liu, P. Han, J. Yao, L. Wang, G. Cui and L. Chen, *ACS Appl. Mater. Interfaces*, 2010, **3**, 93.

[3] X. Zhou, C. Shang, L. Gu, S. Dong, X. Chen, P. Han, L. Li, J. Yao, Z. Liu, H. Xu, Y. Zhu and G. Cui, *ACS Appl. Mater. Interfaces*, 2011, **3**, 3058.

[4] X. Lu, G. Wang, T. Zhai, M. Yu, S. Xie, Y. Ling, C. Liang, Y. Tong and Y. Li, *Nano Lett.*, 2012, **12**, 5376.

[5] D. Choi and P. N. Kumta, *J. Electrochem. Soc.*, 2006, **153**, A2298.